International Journal of Multiphysics
Volume 18, No. 4, 2024
ISSN: 1750-9548

Microencapsulation of Omega-3 from Sage Seed Oil Using Fish Gelatin-Sage seed Gum Complex Coacervation

Khosro Behmaram[1], Aram Bostan[1]*, Ali Dini[2,3], Ghadir Rajabzadeh[1], Ahmad Shaker-Ardakani[4]

[1]Department of Food Nanotechnology, Research Institute of Food Science and Technology (RIFST), Mashhad, Iran.
[2]Pistachio Safety Research Center, Rafsanjan University of Medical Sciences, Rafsanjan, Iran.
[3]Department of Food Sciences and Technology, Faculty of Agriculture, Vali-e-Asr University of Rafsanjan, Rafsanjan, Iran.
[4]Pistachio Research Center, Horticultural Sciences Research Institute, Agricultural Research, Education and Extension Organization (AREEO), Rafsanjan, Iran.
*Corresponding author

Abstract

Omega-3, derived from plant sources, and other bioactive components provide major health advantages mostly because of their antioxidant action. Their poor stability in response to external factors limits their uses. Microencapsulation is one effective way, nonetheless, to protect these fragile molecules and ensure concentrated dispersion. This work used the complex coacervation approach to improve the stability and preservation of omega-3-rich sage seed oil using natural carrier agents like fish gelatin (protein) and sage seed gum (polysaccharide). After optimal pH (4.2), further parameters—zeta potential (-2.56±0.2 mV), particle size (3.12±0.27 µm), and shape—were investigated. The sample with the best formulation performed the best overall. Its loading capacity (93.4±0.85%), microencapsulation yield (95%±0.85), and oxidative stability (3.7±0.11 h) were greatest among others. Microcapsules with irregular shapes and a porous network structure greatly aid to retain omega-3s, according the scanning electron microscopy (SEM) research. The optimized formulation significantly enhanced the dispersion and oxidative stability of omega-3 in food products, making it a suitable candidate for functional applications.

Keywords: Omega-3, Microencapsulation, Complex coacervation, Sage seed oil, Fish gelatin, Oxidative stability, pistachio butter

1. Introduction

Considered generally as beneficial for human health, omega-3 unsaturated fatty acids especially in sufficient quantities include Alpha-linolenic acid among essential fatty acids has to be acquired via food. On public health, however, low omega-3 fatty acid intake is very prevalent and may have negative effects (McClements, 2010). Particularly in fetal and neonatal development, these fatty acids are vital for physiological activities; they have also been proven to lower the risk of cardiovascular disorders, stop blood clots, and slow down inflammation (Saini et al., 2021). Omega-3 fatty acids are generally under-consumed in diet even if they have advantages (Punia et al., 2019). Although omega-3 fatty acids are very important, their inclusion into food items presents major difficulties. Their non-polar character restricts their solubility in water, and their molecular structure is prone to oxidation, which results in disagreeable taste and odor, thereby influencing food quality (Venugopalan et al., 2021). Lipid oxidation reduces dietary value in addition to taste. Thus, many techniques have been investigated to stabilize omega-3s in food items; encapsulation turns out to be the most effective one.

One interesting way to safeguard bioactive molecules is by encapsulating technology. By means of regulated release, this method enhances stability, therefore avoiding oxidation and hence keeping taste (Arenas-Jal et al., 2020). Encapsulation in food systems may be accomplished using many methods including emulsions, biopolymer complexes, and hydrogels, which successfully preserve core ingredients and improve stability (Xie et al., 2023).

Among encapsulating techniques, complex coacervation is notable for generating capsules ranging in size from 1 to 1000 μm. Phase separation—in which active components are enclosed by polymer interactions—forms a stable layer surrounding the core (Muhoza et al., 2022; Napiórkowska & Kurek, 2022). By essentially stopping oil migration to particle surfaces, complex coacervation helps to preserve the organoleptic properties of food goods enhanced with omega-3s during storage (Muhoza et al., 2023).

An ideal encapsulating agent (Chen et al., 2023) fish gelatin is a biocompatible, biodegradable, non-toxic, water-soluble protein with great film-forming capacity. Rich fisheries of Iran provide plenty of chances to create fish gelatin from aquatic waste, thus adding value to byproducts and helping to create bio-based nano-capsules (Amani et al., 2022). Source from Salvia macrosiphon, sage seed gum is also very helpful because of its intrinsic hydrocolloid characteristics, which surround omega-3 fatty acids in a protective coating. The high alpha-linolenic acid concentration of sage seed gum offers nutritional advantages but also increases susceptibility to environmental elements, so it is a suitable coacervation partner for gelatin.

However, a lot of study has been done on omega-3 encapsulation, few studies employing fish gelatin and sage seed gum via complex coacervation. This work intends to create and maximize omega-3-containing coacervates using wall components fish gelatin and sage seed gum. With an eye toward stable omega-3-enriched coacervates fit for food uses, it also assesses the oxidative stability of these coacervates relative to raw sage seed oil. The microcapsules were mixed with pistachio butter and their impacts on sensory, physicochemical qualities, textural profile, and fatty acid content were methodically assessed.

2. Materials and Methods

2.1 Materials

Sage seeds were obtained from local markets in Rafsanjan, Iran. The sage seeds were carefully cleaned to remove chaff, stones, and dust. The mucilage of the sage seeds was extracted using the procedure described by Bostan et al. (2010). Fish gelatin, fatty acid methyl ester (FAME) standards, ammonium thiocyanate, hydrochloric acid, barium chloride dihydrate, and solvents (such as n-hexane, methanol, chloroform, ethanol, and isopropanol) were sourced from Merck, Darmstadt, Germany. Ferrous sulfate heptahydrate and Iron (III) chloride hexahydrate were purchased from Sigma-Aldrich.

2.2 Sage Seed Oil Extraction

Sage seed oil was extracted as described by Bostan et al. (2010). The clean seeds were powdered using a mill, and the powders were mixed with hexane solvent at a ratio of 51:1 (w/v), followed by stirring for 24 hours. The samples were then filtered, and the solvent was evaporated under vacuum using a rotary evaporator at 40 °C (Aram Bostan et al., 2010).

2.3 Analysis of Fatty Acid Composition by Gas Chromatography

The fatty acid content of sage seed oil was ascertained by gas chromatography, whose findings were expressed as relative area percentages. Combining oil with hexane (0.4g in 7mL) with 7mL of 2 N methanolic potassium hydroxide at 50 °C for 20 minutes produced fatty acid methyl esters (FAMEs). Using a gas chromatograph model ACM6000, USA, fitted with Autochrom2000 software, the fatty acid esters were investigated. The system consisted of an ion flame detector and BPX70 silica glass capillary columns (120 m length, 0.22 mm inner diameter, 0.2 μm inner layer thickness). With a flow rate of 17 ml/min, air flow rate of300 ml/min, and hydrogen flow rate of 30 ml/min the carrier gas was helium. Relatively, the oven, injection, and detector temperatures were kept at 198, 250, and 280 °C correspondingly.

Following the coacervation-generated microcapsule enrichment of pistachio butter, the fatty acid profile was once again evaluated using GC to evaluate the new enhanced profile. Consistent with Lim et al. (2010), the initial and final fatty acid profiles of pistachio butter enriched with coacervates containing omega-3 were compared to evaluate the incorporation of omega-3 fatty acids from the sage seed oil; the results were reported based on relative percentage levels.

2.4 Wall Materials

Based on Bostan et al. (2010), a modified technique was followed in extracting sage seed gum. Starting with distilled water, at pH values between 3 and 9 extraction started utilizing water-to---seed ratios ranging from 25:1 to 85:1. A temperature-regulated water bath helped to keep the temperature between 25°C and 80°C after adjusting the pH with 0.1 mol/L NaOH or HCl. Three phases comprised the extraction. Forty grammes of seeds were first submerged in 1000 millilitre of water at the prescribed pH and temperature for twenty-minute. The swelled seeds were then run through an extractor (Model 412, Pars Khazar Co., Iran). Following two further water-soaking cycles, the crude gum was filtered, blended, and overnight dried in a convection oven (Model 4567, Kimya Pars Co., Iran) set at 70°C. Before analysis, the dried gum was crushed and filtered.

2.5 Preparation of FG–SSG Coacervate Phase

100 mL of distilled water at 40°C dissolved exact quantities of FG and SSG. Combining the two solutions in a 1:1 weight ratio of FG to SSG, the overall biopolymer content was 2% (w/v). The pH was changed to 3.5, and as a preservative 0.02% (w/v) sodium azide was added. To enable enough electrostatic interactions between the molecules, the FG–SSG combination was incubated for 24 hours at 40°C under a shaking water bath at 500 rpm.

2.6 Selection of the Complex Coacervation Process:

2.6.1 Preparation of FG-SSG Microcapsules

The effects of FG (Fish Gelatin) and SSG (Sage Seed Gum) on the microencapsulation process were explored to get an ideal formulation for microencapsulation of the core material. Each exact concentration of FG and SSG was dissolved in 100 mL of distilled water set at 40°C. The two solutions were then mixed in a 1:1 weight ratio of FG to SSG, therefore guaranteeing a final biopolymer content of 2% (w/v). The ideal pH for the formulation was found to be 4.2, hence the pH of the combination was changed to that. We added 0.02% (w/v) sodium azide to preserve the solution. To enable enough electrostatic interactions between the molecules, the FG –SSG combination was then incubated at 40°C in a shaking water bath at 500 rpm for 24 hours. Key performance metrics were LC (loading capacity) and MY (microencapsulation yield); encapsulation efficiency was not computed.

2.6.2 Selection of pH

A Zetasizer NanoZS 90 (Malvern Instruments Ltd., UK) was used to track zeta potential values between 3.0 and 7.0 at 25°C. Measuring the electrophoretic mobility of SSG (1% w/w) and FG (1% w/w), the zeta potential was computed using the pertinent conversion formulae. The samples were adequately homogenized using an ultrasonic probe for two minutes before measurement to avoid sedimentation and guarantee homogeneity. The absorbance of a combination of SSG (0.1%) and FG (0.02%) spanning the pH range of 3.0 to 7.0 at 750 nm was simultaneously determined by UV spectrophotometry (1900-TU, Percy General Co., Ltd., Beijing, China). Additionally performed at 600 nm were absorbance measurements for SSG (0.1%, w/w), GA (0.02%, w/w), and many ratios of FG to GA. Based on first turbidity measurements and zeta potential data, the pH at which turbidity was maximized—that which would be the optimal pH for complicated coacervation between SSG and FG—was pH 4.2.

2.6.3 Selection of the FG-to-SSG Ratio

We generated many combinations of SSG and FG at ratios of 1:1, 2:1, 3:1, 4:1, and 5:1; their turbidities were computed by UV spectrophotometer measurement of the light absorbance at 600 nm. The optimal SSG-to- FG ratio matching the highest coacervation yield came out to be the ratio showing the best turbidity and zeta potential stability. To get this ratio, aqueous dispersion comprising SSG and FG was prepared at ambient temperature and pH was adjusted to the optimal value of 4.2. These dispersions were left unchanged over night to allow complex coacervates to form gel-like structure. This step saw the control of coacervate growth and regular monitoring to ensure no appreciable particle aggregation throughout the incubation duration. The dispersions were also gently spun at 100 rpm to preserve consistent dispersion and prevent too much sedimentation.

2.7 Particle Size

Using photon electron spectroscopy under dynamic light scattering, performed with a Zetasizer device (NanoSizer 3000, Malvern Instruments, Malvern, UK), the average particle size and polydispersity index of the complex coacervates were found at a constant scattering angle of 90 degrees.

2.8 Zeta Potential Analysis

The electrostatic stability of the coacervates under varied conditions—such as different gelatin-to---gum ratios and wall-to-- core ratios—was evaluated by measuring the zeta potential of the first emulsions. Using a NanoZS Zetasizer (Malvern Instruments Ltd., Worcestershire, UK), measurements were carried out after a five-fold dilution in line with a previously defined protocol. Reflecting the influence of these factors on the stability of the system, the observed zeta potential values varied from 1.32 ± 0.12 mV to 3.7 ± 0.11 mV.

2.9 Morphology

2.9.1 Morphology Analysis by Light Microscopy

The morphology of protein-polysaccharide mixtures was examined using light microscopy at magnifications of ×10, ×20, and ×40. Samples representing various pH conditions were stirred for 15 minutes at 300 rpm before observation. Aliquots were then withdrawn for immediate analysis.

2.9.2 Morphology Analysis by Scanning Electron Microscopy (SEM)

The FG-SSG coacervate was examined using scanning electron microscopy (FE-SEM TESCAN MIRA3, Czech Republic), operating at an accelerating voltage of 10 kV. Samples were air-dried, mounted on aluminum stubs, and coated with a gold/palladium layer.

2.10 Accelerated Stability Test for Sage Seed Oil Stability Index (OSI) and Coacervated Oil

To evaluate the oxidative stability, 2.5 grams of oil or coacervated oil were tested using the Metrohm Rancimat model 743 at 100°C with an airflow rate of 15 L/h. The oxidative stability index (OSI) was determined by monitoring the induction period.

2.11 Determination of Surface and Total Oil in Microcapsules

0.5 g of microcapsule powder was added into 5 ml hexane, manually agitated for five minutes, then centrifuged at 2000 rpm for five minutes using the SIGMA Laboratory Centrifuge 3-18 (Germany). This determined surface oil. Carefully collected, filtered using Watman 42 paper filter, the resultant supernatant was pipled to a pre-weighed round-bottom flask. Using a rotary evaporator (Hei-VAP; Heidolph Instruments GmbH & Co. KG, Schwabach, Germany) at 60°C, solvent removal was achieved; thereafter, the gravimetric assessment of surface oil was performed using the method outlined by Ifeduba & Akoh (Ifeduba & Akoh, 2016).

To quantify total oil, 2 ml of 5 M HCl was applied to 0.5 g of microcapsule powder for the inner oil release. The mixture was swirled at 60°C for one hour using a magnetic stirrer (RH basic 2; IKA® Works) before let to react at room temperature. The mixture then was moved to a decanter and twice extracted using 5 ml hexane. After filtering the resultant supernatant using Watman 42 paper filter, it was piplined to a pre-weighed round-bottom flask. A rotary evaporator at 60°C helped to remove solvents; gravimetric analysis of total oil was carried out using the technique described by Ifeduba et al. (Ifeduba & Akoh, 2016).

2.12 Microencapsulation Yield and Loading Capacity

The microencapsulation yield (MY) was determined using the following formula:

$$MY = \left(\frac{w2}{w1}\right) \times 100\% \quad (1)$$

Where w1 is the weight of the microcapsules obtained, and w2 is the initial weight of core and wall materials used.The loading capacity (LC) of microcapsules was evaluated by assessing hexane-extractable surface oil and total oil content. The loading capacity was expressed as a percentage, calculated by the difference between total

and surface oil, divided by the mass of the microcapsules. The loading capacity (%) was determined using the formula (Calderón-Oliver et al., 2017):

$$\text{Loading capacity} = \frac{Wt-Ws}{Wm} \times 100 \quad (2)$$

Where W_t and W_s represent the total and surface oil content of the microcapsules, and W_m is the mass (g) of the microcapsules. This calculation provides a quantitative measure of the oil retention capacity of the microcapsules, offering insights into their potential applications in controlled release systems or encapsulation technologies.

2.13 Selection of Coacervation Conditions

Previous research guided the optimization of the coacervation settings for the microencapsulation of omega-3 from sage seed oil. Variations in parameters including pH (4.2), gelatin-to-- gum ratios (2:1 to 4:1), and wall-to--core ratios (1:1 to 4:1) were investigated; zeta potential values ranged from 1.32 ± 0.12 mV to 3.7 ± 0.11 mV, hence confirming electrostatic stability. The procedure Behmaram et al. (2024) was followed in producing pistachio butter employed in this experiment. Coacervates were added at a chosen concentration into the pistachio butter after manufacturing; then, sensory assessment, fatty acid profile, and texture analysis were carried out to evaluate the effects of the microencapsulation on product quality.

2.13.1 Texture Analysis

Texture analysis was performed using the Back Extrusion technique after incorporating coacervates into pistachio butter, with measurements taken at specified time intervals.

2.13.2 Sensory Evaluation

Sensory evaluation was conducted to assess attributes such as taste, smell, firmness, and spreadability of both optimized and control samples on Day 1 and Day 60, using a 5-point hedonic scale.

2.14 Statistical Analysis

All experiments were conducted in triplicate, and results are presented as means ± SD. Statistical significance was determined using one-way ANOVA and Tukey HSD tests (SPSS Ver. 21, $P < 0.05$).

3. Results and Discussion

3.1 Zeta Potential Analysis

Understanding the electrostatic interactions of biopolymers—which are basic in complicated coacervation processes— depends critically on their zeta potentials (Cheng et al., 2023). Figure 1 show the zeta potentials of Fish Gelatine (FG) and Sage Seed Gum (SSG) throughout the pH range of 3.0 to 7.0. FG had a positive zeta potential of 27.80 mV at lower pH levels (pH 3.0), therefore showing a net positive charge on its surface. The zeta potential of FG steadily dropped and finally turned negative (-39.21 mV at pH 7.0 as the pH moved toward neutrality. This discovery marks the point at which FG carries no net charge and conforms with earlier studies (Figure 1). SSG routinely showed a negative zeta potential across all pH levels throughout the studied range, unlike FG (Figure 1). The main charged functions in globular-like random coil architecture inside SSG are carboxylate groups, which explain the negative zeta potential of SSG. Under the circumstances investigated, this property suggests that SSG is an anionic polyelectrolyte (Razavi et al., 2012).

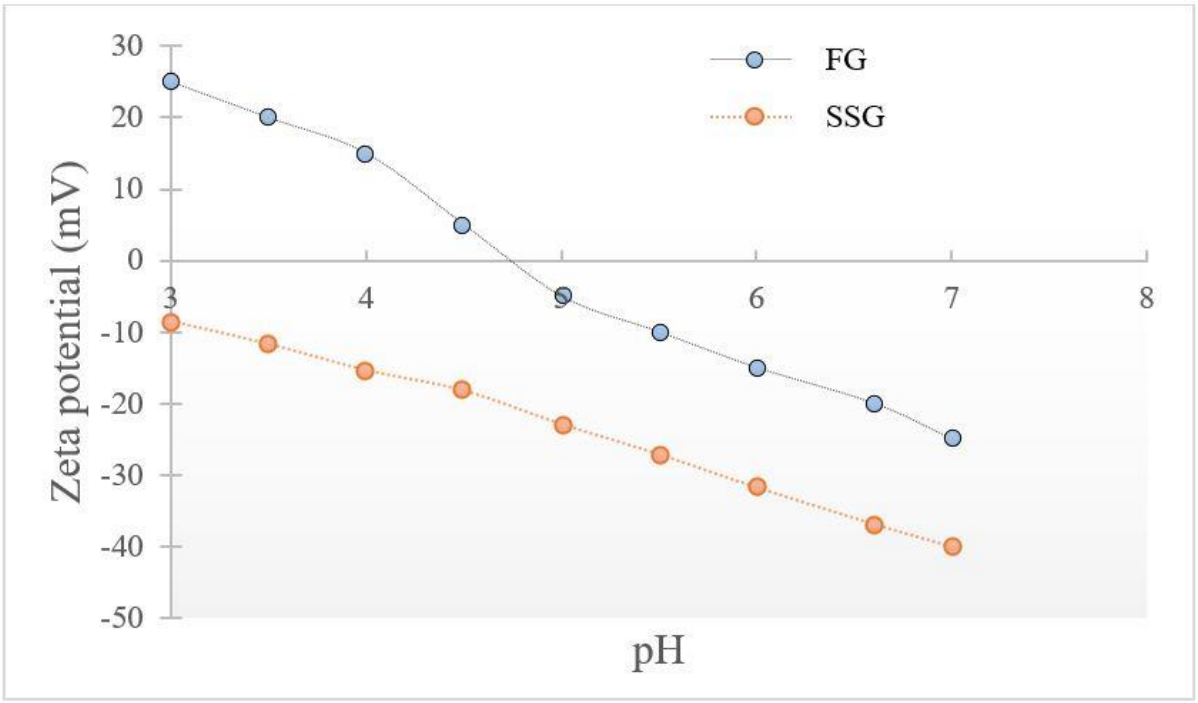

Predicting the behavior of FG and SSG in solution and their inclination to undergo complicated coacervation (Karimi et al., 2013) depend on an awareness of their zeta potentials. Coupled with persistently negative zeta potential of SSG, the change from positive to negative zeta potential for FG as pH rises points to the possibility for favorable electrostatic interactions between these two components. Notwithstanding these differences, the bulk of data clustering around the 4.0 pH mark supports the theory that keeping a pH of around 4.2 might enable good interactions among biopolymers, hence improving the efficiency of the complicated coacervation process (Ru et al., 2012; Weinbreck et al., 2004). Research on complicated coacervation between FG underline the need of knowing zeta potentials for investigating thermodynamic characteristics and phase behavior (Li et al., 2018). Moreover, the invention and choice of complex coacervates including gelatin, cress seed gum, and zedo gum highlight the need of zeta potentials in regulating the complexation process (Gharanjig et al., 2020).

3.2 Impact of pH on Coacervation and Turbidity in FG-SSG Mixtures

In order to support this conclusion, the ideal pH for the development of complex coacervation was found by means of a turbidity test within the pH range of 2.0 to 7.0. Microbial observations, ζ-potential analysis, and turbidity measurements all helped to verify how pH affected coacervation (Dong et al., 2023). Figures 2 show the 600. nm absorbance values of the FG and SSG mixed dispersions. Especially, the development of dense complex coacervates at concentration 0.15, 0.45% w/v in the FG:SSG ratio of 1:1 was seen within the whole pH range with the maximum intensity at pH 4.2. At almost neutral pH, the turbidity for every ratio was almost nil. The turbidity of every concentration rose dramatically as the pH dropped. The turbidity dropped progressively and stabilized at lower pH values when the pH dropped further more. Mixed systems including ovalbumin-GA (Liu et al., 2015), fish gelatin-GA (Yang et al., 2012), and pea protein isolate-GA (Elmer et al., 2011) showed similar trends of turbidity changes during acid titration. In the sodium caseinate-carboxymethyl cellulose system, however, turbidity rose from pH 7 to 2 (Cho et al., 2016) find that more positive charged molecules improve interaction and complex formation due to electroneutrality; this observation is consistent with the figure showing how increasing the concentration of FG-SSG mixtures impacts turbidity. Higher concentrations lead to increased turbidity (De Kruif, Weinbreck, & de Vries, 2004).

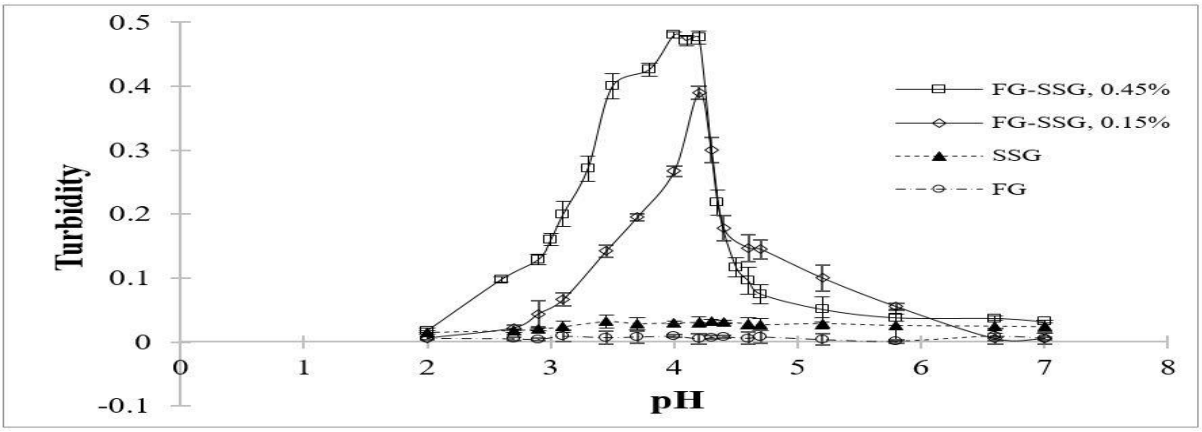

This trend suggests that the interactions between FG and SSG intensify as more positively charged FG molecules interact with SSG at higher pH levels. The turbidity values decrease significantly as the pH approaches 6.0, which aligns with the finding that at this higher pH (above the critical pH of 5.0), the turbidity stabilizes at zero, indicating minimal or no interactions between FG and SSG. This behavior reinforces the conclusion that there is a preferred pH range for effective interaction and complexation.

3.3 Effect of Biopolymer Ratio on Coacervation Behavior at pH 4.2

The charge balance of polyions is much influenced by the interaction between protein and polysaccharide ratios in a mixture, therefore affecting their complexation behavior (Lee, 2008). The ideal pH for several biopolymer combinations is found to be about 4.0, which is in close proximity to the ideal pH of 4.2 found in this work. For a 1:1 biopolymer ratio, for example, gelatin mixed with gum arabic produces an optimal pH of 4.0 (Kaushik & Roos, 2007; Zuanon, Malacrida, & Telis, 2013). At a biopolymer ratio of 2:1 (Coacervates; Weinbreck et al., 2004) , whey protein combined with gum arabic also showed an optimal pH of 4.0. These results imply that formulations with a pH close to 4.2, including those using a gelatin-to-- gum ratio of 3:1, are probably going to show good coacervation properties. Other biopolymers such as gum arabic and chitosan combined,

Clearly in Figure 3 the maximum absorbance value occurred at a FG-to-- SSG ratio of 3:1, suggesting increased turbidity brought about by electrostatic interactions between FG and SSG. We examined the yield of complex coacervates at many FG-to-- SSG ratios to support this conclusion; the related data is shown in Figure 3. Aligning with the turbidity data, the maximal coacervate production of 75.2% was attained at the FG-to-- SSG ratio of 3:1 (Figure 3). Reduced coacervate yields produced by other FG-to---SSG ratios indicated the possible synthesis of soluble complexes rather than insoluble ones.

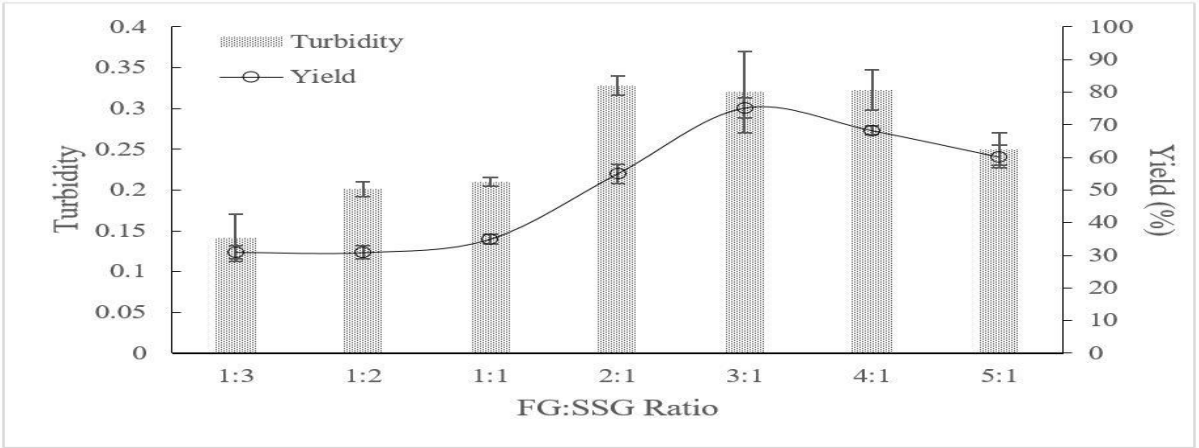

The biopolymer ratio and pH of the dispersion (X. Li, Su, Han, Yan, & Sun, 2023), define elements changing the charge density of the complexes. The electrostatic interaction between FG and SSG shown in two different phases

at pH 4.2 and a 3:1 ratio. This phenomena results from the synthesis of biopolymers with several soft, dense coacervate phase and a dilute phase marked by reduced biopolymer concentrations.

3.4 Light Microscopy Analysis of Coacervates

Important new perspectives on the intricate coacervate production process and its absorption onto oil droplets were offered by optical microscopy Figure 4A shows above the isoelectric point (IEP) of FG (≈5.4) no clear complex coacervates are seen on oil droplets. Strong repulsion between negatively charged FG and Sage Seed Gum (SSG) at this pH limits coacervate formation, therefore reducing the circumstances suitable for encapsulation via like-charged particle repulsion and steric hindrance. By contrast, significant changes occur as the dispersion pH approaches the IEP of FG (≈4.7), as seen in Figure 4B. Reduced resistance between FG and SSG helps oil droplets assemble, helped by diminished electrostatic repulsion when FG's surface charge approaches neutrality. Furthermore, steric repulsion between droplets is not enough to prevent aggregation; thus, attractive interactions among biopolymer molecules—van der Waals and hydrophobic forces—allow bigger clusters of oil droplets to form. Complex coacervates in the continuous phase when the pH drops even further below the IEP (Figure 4C), with coacervates moving to create a clear layer surrounding the oil droplets. The positively charged FG interacts with the negatively charged SSG to enable this activity; so, FG becomes positively charged below its IEP. Usually at the isoelectric point (IEP) of the protein, the pH ideal for coacervate production is Proteins get a positive charge below the IEP, therefore encouraging electrostatic interactions with negatively charged polysaccharides and enabling sustained coacervate formation. Reducing pH too much, however, might cause charge reversal and repulsion between positively charged proteins, therefore impairing complex stability (Hu et al., 2019) (Wang, 2020). All things considered, microcapsule development is much influenced by pH circumstances. Positively charged proteins improve coacervate production and encapsulation under the IEP. By contrast, repulsive forces hinder the process above the IEP, producing less coacervates on oil droplets (Vargas, Delgado-Macuil, Ruiz-Espinosa, Rojas-López, & Amador-Espejo, 2021).

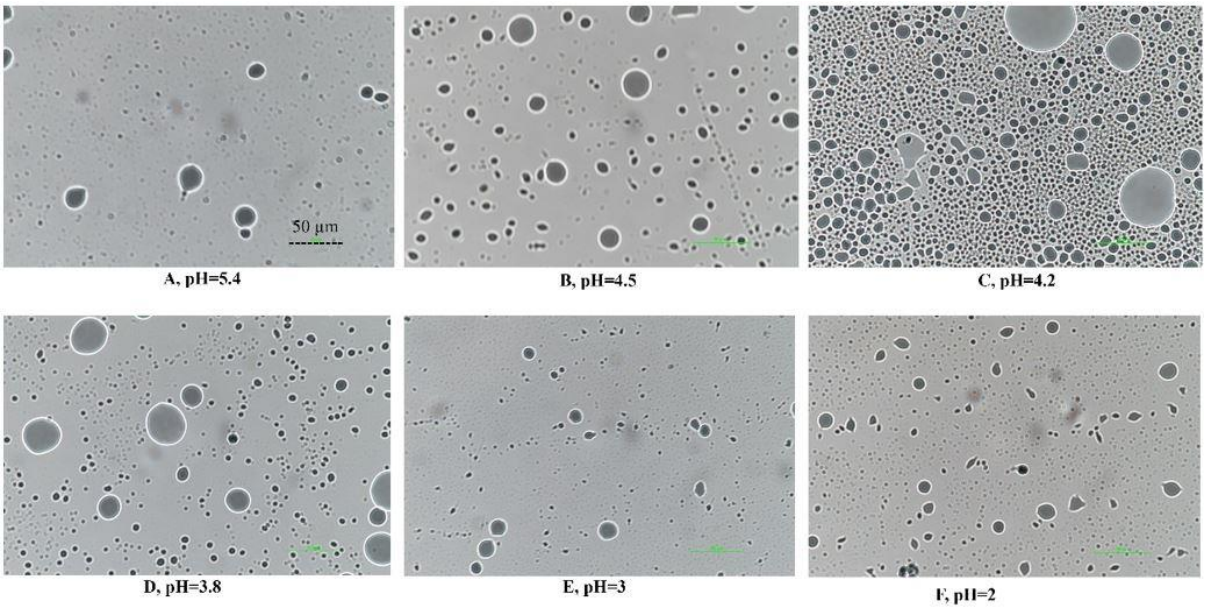

3.5 Microencapsulation Yield and Loading Capacity

Table 1 presents features of coacervates on the path of selecting a good sample o enhance pistachio butter.The loading capacity (LC) of the microcapsules ranging from 75.2% to 93.4% is mainly influenced in this work by wall-to-- core ratios, concentration of sage seed oil, and FG-to- -- SSG ratios. With a 3:1 fish gelatin (FG) to sage seed gum (SSG) ratio, the highest LC noted was 92.5%. Effective interaction between fish gelatin and sage seed gum at this ideal ratio helps to explain this larger loading capacity given a strong encapsulating matrix that promotes oil retention and encapsulating efficiency. Larger particles produced by the combination of wall-to--- core ratio and high FG-to--- SSG ratio help to limit surface oil consumption and increase core material retention.

Larger particles especially help to resist oxidation, hence enhancing the stability and sensory quality of the encapsulated oil (Jafari, He, & Bhandari, 2007; Yun, Devahastin, & Chiewchan, 2021).

Table 1. Investigating the properties of coacervates containing sage seed oil.

Wall: Core Ratio	FG:SSG Ratio	Size (µm)	Zeta potentioal (-)	PDI	LC	MY	OSI (100°C)
1:1	2:1	0.721±0.05^{a}	4.02±0.42^{def}	0.435±0.035^{de}	75.2±0.5^{a}	82±0.5 ^{a}	1.32±0.12^{a}
1:1	3:1	2.937±0.19^{d}	2.48±0.42^{abc}	0.361±0.024^{d}	78.3±0.6^{ab}	85±0.6 ^{b}	1.72±0.05^{b}
1:1	4:1	2.439±0.25^{dc}	3.62±0.2^{d}	0.466±0.21^{e}	77.4±0.9^{a}	84.2±0.9 ^{a}	1.8±0.1^{b}
2:1	2:1	2.154±0.14^{c}	2.11±0.15^{b}	0.22±0.031^{c}	77.3±0.8^{a}	84±0.8 ^{a}	2.1±0.29^{bc}
2:1	3:1	0.842±0.08^{ab}	4.54±0.16^{e}	0.082±0.035^{ab}	80.1±1.12^{b}	87±1.12 ^{b}	2.42±0.15^{c}
2:1	4:1	1.254±0.33^{bc}	5.31±0.18^{f}	0.142±0.015^{b}	84.1±2.95a^{bc}	90±2.95 ^{c}	2.51±0.06^{c}
3:1	2:1	1.321±0.29^{bc}	2.15±0.14^{b}	0.03±0.022^{a}	86.4±1.31^{c}	91±1.31 ^{d}	2.6±0.19^{cd}
3:1	3:1	0.987±0.1^{b}	2.82±0.19^{c}	0.043±0.017^{a}	84.7±.74b^{c}	89.4±0.74 ^{d}	2.77±0.11^{d}
3:1	4:1	3.296±0.32^{de}	1.32±0.18^{a}	0.217±0.043^{bc}	87.3±0.65^{c}	92±0.65 ^{d}	2.9±0.2^{d}
4:1	2:1	2.12±0.18^{c}	3.67±0.21^{d}	0.168±0.015^{b}	89.7±1.85^{dc}	93±1.85 ^{e}	3.13±0.17^{de}
4:1	3:1	3.12±0.27d^{e}	2.56±0.2^{bc}	0.062±0.029^{ab}	93.4±0.85^{d}	95±0.85^{f}	3.7±0.11^{e}
4:1	4:1	3.78±0.51^{e}	1.35±0.12^{a}	0.04±0.019^{a}	92.5±0.5^{d}	94.5±0.5^{f}	3.6±0.2^{e}

With LC values as high as 92.5%, the findings of this research much surpass those of prior studies on microencapsulation of oils, including Kanha et al. (2021), where the LC for freeze-dried microcapsules was recorded from 31.9% and 34.5%. The higher values reported here imply that the fish gelatin-SSG combination has better encapsulating qualities.

In accordance with the LC, the yield (MY) in this work also showed positive results, meaning that the approach of encapsulating the FG-SSG not only improves oil retention but also reduces the loss of the encapsulated material during processing. Confirming that greater wall material concentrations resulted in better encapsulation and lower surface oil, the wall-to-- core ratio proved to be vital in increasing both MY and LC, thereby strengthening the general stability of the product (Carneiro, Tonon, Grosso, & Hubinger, 2013).

Studies showing comparable outcomes when raising wall-to-- core ratios also corroborate this, particularly when using natural gums and gelatin-based systems. For various seed gums, notably chia and basil, encapsulation efficiency (EE%) values ranging from 70% to 88% have been recorded, thereby further confirming the usage of these natural polymers for attaining high LC (Akcicek, Bozkurt, Akgül, & Karasu, 2021) .

Furthermore, as previous research have demonstrated, LC and encapsulation performance depend much on the particle size. Like the results of Mu et al. (2024), where protein-polysaccharide systems increased oil retention and stability by lowering surface oil concentration, larger particles generated at higher FG-to-- SSG ratios connected with greater encapsulation efficiency (Mu, Hu, Tang, Dong, & Zhang, 2024).

3.6 Oil Stability and Oxidative Resistance Analysis

Depending on elements like content of fatty acids, availability of antioxidants, as well as initial quality indicators including acid value (AV), peroxide value (PV), and processing technique (Dini, Falahati-pour, & Hashemipour, 2023), the Oil Stability Index (OSI) of Sage seed oil at 100°C might vary. Because of their rich polyunsaturated fatty acid (68.4% PUFAs), which are prone to oxidation, Sage seed generally has a somewhat low OSI when

compared to certain other oils. Nonetheless, depending on the particular composition and quality of the oil, OSI values for SSO might vary from one hour to almost three hours at 98°C (Bostan, Mohebbi, Khodaparast, Varidi, & Nikooei, 2013), Sage seed generally has a somewhat low OSI when compared to certain other oils. Nonetheless, depending on the particular composition and quality of the oil, OSI values for SSO might vary from one hour to almost three hours at 98°C (Ma, Zhao, Wang, & Sun, 2019). During the choice of the coacervation technique, seeing the OSI coacervate index might be very beneficial. It helps evaluate whether the coacervate production helps maintain the oxidative stability of the encapsulated Omega-3. Furthermore, it acts as a quality control factor during microcapule manufacturing so that the intended protective action against oxidation is always obtained. From 1.32 to 3.7 h in treatments, Table 1 also offers a thorough summary of the oil stability index of coacervates including sage seed oil (SSO). These findings provide important new directions on the stability of encapsulated omega-3 from sage seed oil and the oxidative resilience of microcapsules. Emphasizing the efficiency of this technique in improving oxidative stability, sage seed oil coacervation notably greatly raised the OSI100°C from 1.1 h (Cold press SSO, Table 1) to 3.7 h in coacervated SSO. Consistent values of the OSI show the effect on oxidative stability of the wall-to---core ratio and the fish gelatin to Sage seed gum ratio. Due to the positive charge of fish gelatin improving interactions with polyphenolic chemicals in sage seed oil, thereby giving a protective effect against oxidation, increasing the gelatin-to-- gum ratio helps to enhance oxidative stability Concurrently, a greater wall-to---core ratio results in higher OSI values, indicating improved oxidative stability, which fits the idea that a higher concentration of wall material better protects encapsulated omega-3 fatty acids from external influences favoring oxidation (Perez-Palacios et al., 2022).

Loading capacity (LC) and the oxidative stability index (OSI) are crucial parameters assessed to evaluate the efficiency of omega-3 microencapsulation (Tamjidi, Nasirpour, & Shahedi, 2013). Crucially evaluated to determine omega-3 microencapsulation's efficacy are loading capacity (LC) and the oxidative stability index (OSI). OSI and LC exhibit a positive link wherein increasing LC increases OSI, therefore highlighting the ability of coacervates to capture and preserve omega-3 from sage seed oil. Fascinatingly, OSI index values—which indicate microcapsule oxidative resistance—show a similar tendency. Reduced OSI results indicate that cooperatively with a greater gelatin-to---gum ratio and a higher wall-to---core ratio has better oxidative resistance. This association emphasizes the need of taking loading capacity and oxidative resistance into account when assessing microencapsulation effectiveness for systems of omega-3 administration (Habibi, Keramat, Hojjatoleslamy, & Tamjidi, 2017).

3.7 Morphology of microcapsules (SEM)

The structure and appearance of the best microcapsules were assessed using scanning electron microscopy (SEM) examination. Typical of the freeze-drying technique, the SEM micrographs show that the microcapsules have uneven surfaces and irregular forms, which may improve the encapsulation effectiveness of omega-3 oils by raising the contact surface area. These surface flaws, however, may potentially cause increased release rates, which would call for more choice. As observed by Nickerson, Yan, Cloutier, and Zhang (2014), the combination of fish gelatin (FG) with sage seed gum (SSG) generates a macromolecular network that results in a porous structure featuring vacuoles that function as encapsulation sites for the oil). Especially, our findings reveal a good association between oxidative stability index (OSI) and loading capacity (LC), thus showing good omega-3 retention.

Furthermore, the very porous surface structure improves interior space for oil encapsulation, in line with observations of higher loading of bioactive chemicals in comparable systems made by Santos et al. (2015). Moreover, increasing the wall-to-core ratio enhances oxidative stability .The phase-separated shape, in which SSG has denser appearance and FG forms linked clusters, represents the different physical characteristics of the biopolymers, therefore supporting observations by Tan et al. (2018). A balance of porosity and stability is verified to depend on a FG-to-- SSG ratio of 3:1.(Alves, Messaoud, Desobry, Costa, & Rodrigues, 2016) .The phase-separated morphology, where FG forms interconnected clusters and SSG appears denser, reflects the differing physical properties of the biopolymers, corroborating findings by Tan et al. (2018). A FG-to-SSG ratio of 3:1 is confirmed as essential for achieving a balance of porosity and stability.

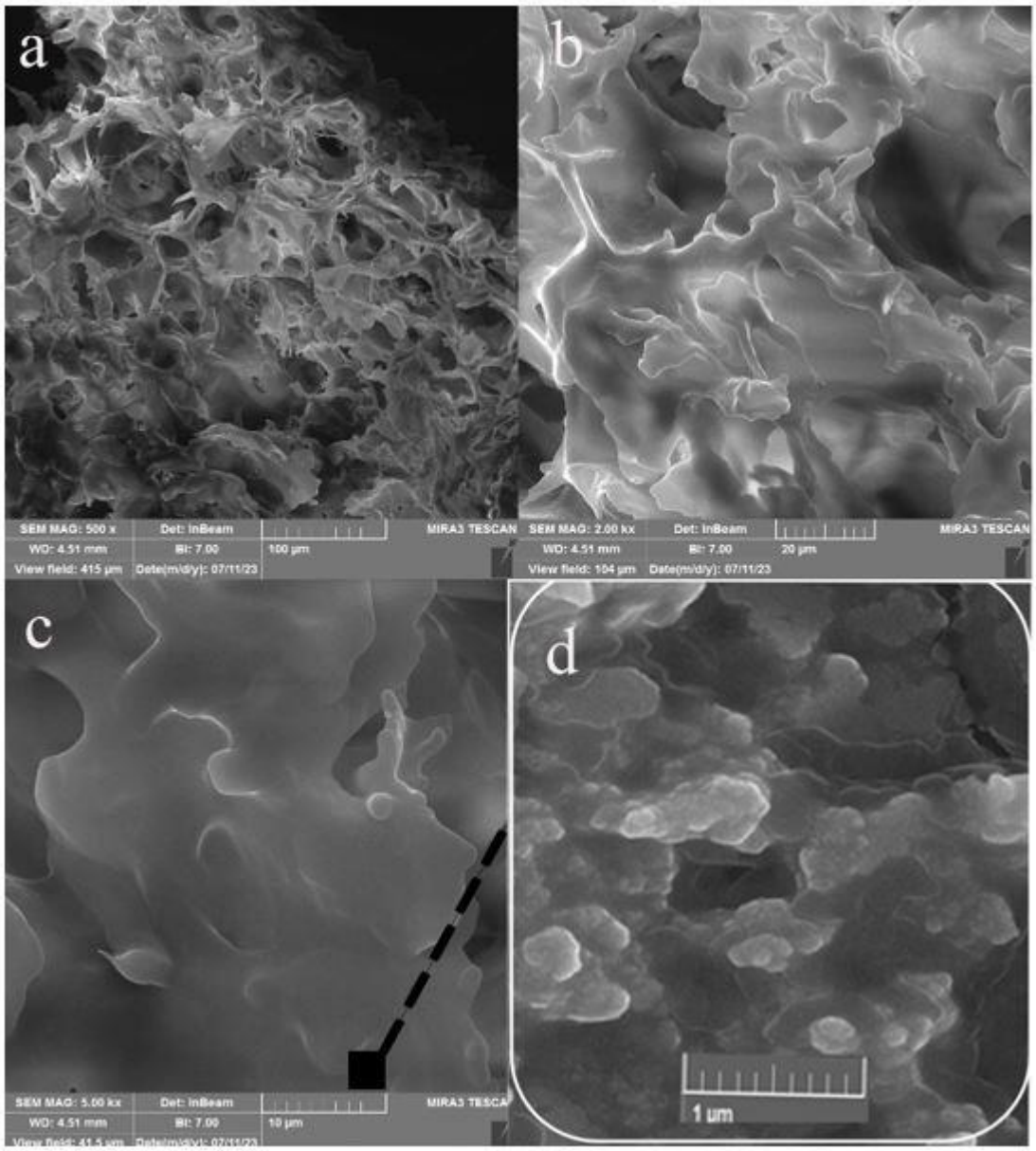

Characterized by irregular forms, porous structures, and prominent phase separation, the SEM pictures show effective coacervation under optimal circumstances (pH 4.2 and FG-to--SSG ratio of 3:1) (Figure 5). Although this shape may help release rates, it also makes long-term stability difficult and suggests the need of more research on drying techniques or wall materials to improve microcapsule uniformity and mechanical properties (Espinosa-Andrews, Sandoval-Castilla, Vázquez-Torres, Vernon-Carter, & Lobato-Calleros, 2010; Fonte et al., 2012).

3.8 Texture analysis

Table 2 lists the results of texture examination of the piston butter samples. The best sample had much higher values for both than the control sample, which measured 1373.062 g.sec for hardness and 14370.915 g.sec for cohesion. The stickiness of both samples was modest; the ideal sample exhibited somewhat greater stickiness (0.062 g.sec) than the control (0.039 g.sec).These findings reveal that adding coacervates considerably enhances the textural characteristics of the pistachio butter. Microencapsulation of omega-3 fatty acids tends to improve the structural integrity of the butter by increasing the increased hardness and cohesiveness in the ideal sample, thereby generating a more pleasant mouthfeel and stability. The low stickiness seen in both samples is advantageous for consumer acceptance and highlights the efficiency of coacervation as a means of optimizing functional food compositions.

Table 2. Effect of Coacervates on Textural Properties of Pistachio Butter Samples.

Sample	Firmness (g.sec)	Cohesiveness (g.sec)	Stickiness (g.sec)
Control	1373.062±59.7643	14370.915±0.915	0.039±0.10329
optimized	2061.213±213.52	22611.532±11.532	0.062±0.1373

3.9 Fatty Acid Composition by Gas Chromatography

Against traditional pistachio butter (0.2±0.01%), Table 3 indicates the significant increase in omega-3 fatty acids (C18:3n3) in pistachio butter improved with sage seed oil (2.13±0.02%). Although a good meal, normal pistachio butter contains only very low quantities of omega-3, which is insufficient daily consumption. Rich in omega-3, fish gelatin-sage seed gum coaculates and sage seed oil helps to significantly increase the omega-3 content and oxidative stability of the resulting pistachio butter. This outcome conforms to the 2010 evaluation of Deckelbaum and Torrejon on the challenges in improving diets with omega-3 fatty acids. They noted that efforts in the food industry have to incorporate not only customer acceptance but also lipid oxidation, which may be lowered with excellent processing methods such microencapsulation(Jacobsen, 2010). Furthermore underscored by Saini et al. (2021) recently identified plant and microbial sources of omega-3 PUFAs, including sage seed oil, which provides a more stable and bioavailable form than traditional sources (Saini et al, 2021). Their study highlights the growing need of consumers for plant-based omega-3 sources, especially if they assist to prevent chronic metabolic illnesses. The enhanced pistachio butter matches these developments and provides a reasonable, nutritionally superior alternative that meets global dietary requirements for omega-3 intake with its greater omega-3 content. Providing a sustainable replacement for fish-based sources of omega-3, the improved pistachio butter might help men (1.6 g) and women (1.1 g) meet their daily omega-3 nutritional requirements (Saini et al., 2021).

Table 3. Fatty Acid Composition of Sage Seed Oil, Regular Pistachio Butter, and Omega-3 Enriched Pistachio Butter.

Fatty acid type		Sage seed oil	pistachio butter%	Pistachio butter enriched
SFA	C12:0	0.014±0.008	-	-
	C14:0	0.058±0.01	0.09±0.02	0.06±0.02
	C16:0	8.83±0.85	9.13±0.62	8.79±0.52
	C17:0	0.16±0.06	0.05±0.01	0.05±0.02
	C18:0	2.32±0.12	1.65±0.12	1.60±0.08
	C20:0	0.10±0.04	0.03±0.01	0.05±0.01
	C22:0	0.064±0.01	0.14±0.04	0.17±0.04
	C24:0	0.0473±0.01	0.05±0.01	0.05±0.01
MUFA	C16:1	0.2±0.02	0.96±0.03	0.83±0.02
	C17:1	0.059±0.02	-	-
	C18:1	23.95±1.02	57.8±1.01	53.89±1.5
PUFA	C18:2	24.07±0.82	28.86±0.97	29.79±1.04
	C18:3 (w6)	0.093±0.01	0.71±0.03	0.42±0.01
	C18:3n3 (w3)	44.48±1.32	0.2±0.01	2.13±0.02

3.10 Sensory evaluation

Table 4 presents over a 60-day period the organoleptic evaluation of pistachio butter enriched with microencapsulated omega-3 using sag seed gum and fish gelatin. According to the sensory investigation, taste and mouthfeel remained quite steady but certain characteristics, like appearance of oiliness and rigidity, clearly changed over time.

The little decline in the flavor ratings in the enriched and control samples implies that adding omega-3 microcapsules had no meaningful influence on the overall taste character of the pistachio butter. This suggests that the coacervation method was effective in reducing omega-3 oxidation, often associated with unpleasant sensory changes. Similarly, the mouthfeel maintained its integrity throughout time, particularly in the enhanced sample, therefore confirming that the microcapsules had no detrimental influence on the texture of the product. Particularly by Day 60, traits like oiliness in appearance and hardness showed more obvious changes. Both samples felt less greasy presumably from structural changes in the encapsulated fat. Still, the upgraded sample's improved and more constant stiffness suggested improved textural retention when compared to the control.

Microencapsulated omega-3 added to pistachio butter proved to be generally successful as the product remained appetizing over time. Especially in taste and texture, the coacervation process effectively combined omega-3 without substantial reduction in organoleptic properties, therefore enhancing the nutritional profile of pistachio butter.

Table 4. Sensory evaluation analysis.

Attribute	**Sample**	**Day 1**	**Day 60**
Taste	Optimized	4.5a±0.2	4.4b±0.3
	Control	4.9a±0.1	4.5b±0.1
Smell	Optimized	4.5a±0.3	4.2a±0.1
	Control	4.3a±0.3	4.3a±0.1
Oily Appearance	preferred	4.2a±0.3	3.8b±0.3
	Control	4.1a±0.2	3.6b±0.3
Firmness	preferred	4.6a±0.1	4.4b±0.2
	Control	3.8a±0.4	3.5b±0.5
Mouthfeel	preferred	4.7a±0.3	4.6b±0.1
	Control	4.3a±0.3	4.4a±0.1
Spreadability	preferred	4.0a±0.12	3.8b±0.3
	Control	4.1a±0.1	3.8b±0.1
Graininess	preferred	3.2a±0.4	3.4a±0.2
	Control	4.4a±0.1	4.3a±0.1
	preferred	4.8a±0.2	4.4b±0.1

Overall Acceptance	Control	4.5a±0.1	4.4b±0.4

4. Conclusion

This study focused on the manufacture of omega-3-rich microcapsules by means of advanced coacervation using sage seed gum and fish gelatin as encapsulating agent. Key elements investigated for effective encapsulation were pH, FG-to----SSG ratio, wall-to-----core ratio, and loading capacity. Microencapsulation was found to be optimal at pH 4.2, afg-to----SSG ratio of 3:1; this generated high microencapsulation yield (95% ± 0.85%) and loading capacity (93.4±0.85%). SEM study confirmed microcapsule irregular shape and porous network structure. The omega-3 retention was found to be quite constant given a significant increase in oxidative stability (OSI = 3.7±0.11 h). Over 60 days, successful inclusion of the microencapsulated oil into a food sample—pistachio butter—improved its fatty acid profile and texture and maintained excellent sensory appeal. These findings indicate how effectively complex coacervation may produce stable and bioactive omega-3 microcapsules for application in functional meals.

CRediT authorship contribution statement: Khosro Behmaram: Methodology, Validation, Formal analysis, Data curation, Writing – original draft. **Ali Dini:** Conceptualization, Investigation, Methodology, Data curation, Formal analysis, Writing–original draft, Writing–review & editing, Supervision. **Aram Bostan:** Conceptualization, Supervision, Project administration, Writing – review & editing, Resources. **Ghadir Rajabzadeh:** Conceptualization, Methodology, Formal analysis, Writing – review & editing. **Ahmad shker-Ardakani:** Conceptualization, Methodology, Formal analysis, Writing – review & editing.

Data Availability: Data will be made available on request.

Acknowledgements: The authors would like to thank Rafsanjan University of Medical Sciences, Rafsanjan, Iran, for supporting this study.

Funding: This study is financially supported by Rafsanjan University of Medical Sciences (RUMS) under I.R.'s ethical code. RUMS. REC.1402.165 at RUMS.

Conflict of interest: The authors declare that they have no conflict of interest.

Ethical approval: This article includes no study on human participants or animals as performed by any authors.

References

1. Akcicek, A., Bozkurt, F., Akgül, C., & Karasu, S. (2021). Encapsulation of olive pomace extract in rocket seed gum and chia seed gum nanoparticles: Characterization, antioxidant activity and oxidative stability. *Foods*, *10*(8), 1735.
2. Alves, N. N., Messaoud, G. B., Desobry, S., Costa, J. M. C., & Rodrigues, S. (2016). Effect of drying technique and feed flow rate on bacterial survival and physicochemical properties of a non-dairy fermented probiotic juice powder. *Journal of food engineering*, *189*, 45-54.
3. Bostan, A., Mohebbi, M., Khodaparast, M., Varidi, M., & Nikooei, B. (2013). Study the fatty acid composition and the physicochemical properties of Salvia macrosiphon Boiss seed oil. *Iranian Food Science & Technology Research Journal*, *9*(3).
4. Calderón-Oliver, M., Pedroza-Islas, R., Escalona-Buendía, H. B., Pedraza-Chaverri, J., & Ponce-Alquicira, E. (2017). Comparative study of the microencapsulation by complex coacervation of nisin in combination with an avocado antioxidant extract. *Food Hydrocolloids*, *62*, 49-57.
5. Carneiro, H. C., Tonon, R. V., Grosso, C. R., & Hubinger, M. D. (2013). Encapsulation efficiency and oxidative stability of flaxseed oil microencapsulated by spray drying using different combinations of wall materials. *Journal of food engineering*, *115*(4), 443-451.
6. Cheng, C., Tu, Z., & Wang, H. (2023). pH-induced complex coacervation of fish gelatin and carboxylated chitosan: Phase behavior and structural properties. *Food Research International*, *167*, 112652.

7. Cho, H., Jung, H., Lee, H., Kwak, H. K., & Hwang, K. T. (2016). Formation of electrostatic complexes using sodium caseinate with high-methoxyl pectin and carboxymethyl cellulose and their application in stabilisation of curcumin. *International Journal of Food Science & Technology*, *51*(7), 1655-1665.
8. Coacervates, G. A. Rheological Properties of Whey Protein/Gum Arabic Coacervates. *Whey protein/polysaccharide coacervates: structure and dynamics*, 109.
9. De Kruif, C. G., Weinbreck, F., & de Vries, R. (2004). Complex coacervation of proteins and anionic polysaccharides. *Current opinion in colloid & interface science*, *9*(5), 340-349.
10. Dini, A., Falahati-pour, S. K., & Hashemipour, H. (2023). Oxidation kinetic studies of virgin and solvent extracted pistachio oil under Rancimat test conditions. *Journal of Food Measurement and Characterization*, *17*(1), 653-663.
11. Dong, Z., Yu, S., Zhai, K., Bao, N., Rashed, M. M., & Wu, X. (2023). Fabrication and Characterization of Complex Coacervation: The Integration of Sesame Protein Isolate-Polysaccharides. *Foods*, *12*(19), 3696.
12. Elmer, C., Karaca, A. C., Low, N. H., & Nickerson, M. T. (2011). Complex coacervation in pea protein isolate–chitosan mixtures. *Food Research International*, *44*(5), 1441-1446.
13. Espinosa-Andrews, H., Sandoval-Castilla, O., Vázquez-Torres, H., Vernon-Carter, E. J., & Lobato-Calleros, C. (2010). Determination of the gum Arabic–chitosan interactions by Fourier Transform Infrared Spectroscopy and characterization of the microstructure and rheological features of their coacervates. *Carbohydrate polymers*, *79*(3), 541-546.
14. Fonte, P., Soares, S., Costa, A., Andrade, J. C., Seabra, V., Reis, S., & Sarmento, B. (2012). Effect of cryoprotectants on the porosity and stability of insulin-loaded PLGA nanoparticles after freeze-drying. *Biomatter*, *2*(4), 329-339.
15. Gharanjig, H., Gharanjig, K., Hosseinnezhad, M., & Jafari, S. M. (2020). Development and optimization of complex coacervates based on zedo gum, cress seed gum and gelatin. *International journal of biological macromolecules*, *148*, 31-40.
16. Habibi, A., Keramat, J., Hojjatoleslamy, M., & Tamjidi, F. (2017). Preparation of fish oil microcapsules by complex coacervation of gelatin–gum arabic and their utilization for fortification of pomegranate juice. *Journal of Food Process Engineering*, *40*(2), e12385.
17. Hu, J., Zhao, T., Li, S., Wang, Z., Wen, C., Wang, H., . . . Ji, C. (2019). Stability, microstructure, and digestibility of whey protein isolate–Tremella fuciformis polysaccharide complexes. *Food Hydrocolloids*, *89*, 379-385.
18. Ifeduba, E. A., & Akoh, C. C. (2016). Microencapsulation of stearidonic acid soybean oil in Maillard reaction-modified complex coacervates. *Food Chemistry*, *199*, 524-532.
19. Jacobsen, C. (2010). Enrichment of foods with omega-3 fatty acids: a multidisciplinary challenge. *Annals of the New York Academy of Sciences*, *1190*(1), 141-150.
20. Jafari, S. M., He, Y., & Bhandari, B. (2007). Role of powder particle size on the encapsulation efficiency of oils during spray drying. *Drying Technology*, *25*(6), 1081-1089.
21. Kanha, N., Regenstein, J. M., & Laokuldilok, T. (2022). Optimization of process parameters for foam mat drying of black rice bran anthocyanin and comparison with spray-and freeze-dried powders. *Drying Technology*, *40*(3), 581-594.
22. Karimi, F., Qazvini, N. T., & Namivandi-Zangeneh, R. (2013). Fish gelatin/laponite biohybrid elastic coacervates: a complexation kinetics–structure relationship study. *International journal of biological macromolecules*, *61*, 102-113.
23. Kaushik, V., & Roos, Y. H. (2007). Limonene encapsulation in freeze-drying of gum Arabic–sucrose–gelatin systems. *LWT-Food Science and Technology*, *40*(8), 1381-1391.
24. Lee, J. (2008). *Physical properties of polysaccharides and their interactions with protein at multi-length scales*: Rutgers The State University of New Jersey, School of Graduate Studies.
25. Li, X., Su, Y., Han, X., Yan, Q., & Sun, Q. (2023). Effects of biopolymer ratio and pH value on the complex formation between whey protein isolates and soluble Auricularia auricular polysaccharides. *Food Science of Animal Products*.

26. Li, Y., Zhang, X., Zhao, Y., Ding, J., & Lin, S. (2018). Investigation on complex coacervation between fish skin gelatin from cold-water fish and gum arabic: Phase behavior, thermodynamic, and structural properties. *Food Research International, 107*, 596-604.
27. Liu, J., Shim, Y. Y., Wang, Y., & Reaney, M. J. (2015). Intermolecular interaction and complex coacervation between bovine serum albumin and gum from whole flaxseed (Linum usitatissimum L.). *Food Hydrocolloids, 49*, 95-103.
28. Ma, T., Zhao, H., Wang, J., & Sun, B. (2019). Effect of processing conditions on the morphology and oxidative stability of lipid microcapsules during complex coacervation. *Food Hydrocolloids, 87*, 637-643.
29. McClements, D. J. (2010). Emulsion design to improve the delivery of functional lipophilic components. *Annual review of food science and technology, 1*, 241-269.
30. Mu, J., Hu, R., Tang, Y., Dong, W., & Zhang, Z. (2024). Microencapsulation of green coffee oil by complex coacervation of soy protein isolate, sodium casinate and polysaccharides: Physicochemical properties, structural characterisation, and oxidation stability. *International journal of biological macromolecules, 256*, 128064.
31. Perez-Palacios, T., Ruiz-Carrascal, J., Solomando, J. C., De-la-Haba, F., Pajuelo, A., & Antequera, T. (2022). Recent Developments in the Microencapsulation of Fish Oil and Natural Extracts: Procedure, Quality Evaluation and Food Enrichment. *Foods, 11*(20), 3291.
32. Punia, S., Sandhu, K. S., Siroha, A. K., & Dhull, S. B. (2019). Omega 3-metabolism, absorption, bioavailability and health benefits–A review. *PharmaNutrition, 10*, 100162.
33. Razavi, S. M., Moghaddam, T. M., Emadzadeh, B., & Salehi, F. (2012). Dilute solution properties of wild sage (Salvia macrosiphon) seed gum. *Food Hydrocolloids, 29*(1), 205-210.
34. Ru, Q., Wang, Y., Lee, J., Ding, Y., & Huang, Q. (2012). Turbidity and rheological properties of bovine serum albumin/pectin coacervates: Effect of salt concentration and initial protein/polysaccharide ratio. *Carbohydrate polymers, 88*(3), 838-846.
35. Saini, R. K., Prasad, P., Sreedhar, R. V., Akhilender Naidu, K., Shang, X., & Keum, Y.-S. (2021). Omega− 3 polyunsaturated fatty acids (PUFAs): Emerging plant and microbial sources, oxidative stability, bioavailability, and health benefits—A review. *Antioxidants, 10*(10), 1627.
36. Shariat, S., Hakimzadeh, V., & Pardakhty, A. (2020). The physicochemical and organoleptic evaluation of the nano/micro encapsulation of Omega-3 fatty acids in lipid vesicular systems. *Nanomed J, 7*(1), 80-86.
37. Tamjidi, F., Nasirpour, A., & Shahedi, M. (2013). Mixture design approach for evaluation of fish oil microencapsulation in gelatin-acacia gum coacervates. *International Journal of Polymeric Materials and Polymeric Biomaterials, 62*(8), 444-449.
38. Vargas, S. A., Delgado-Macuil, R.-J., Ruiz-Espinosa, H., Rojas-López, M., & Amador-Espejo, G.-G. (2021). High-intensity ultrasound pretreatment influence on whey protein isolate and its use on complex coacervation with kappa carrageenan: Evaluation of selected functional properties. *Ultrasonics sonochemistry, 70*, 105340.
39. Venugopalan, V. K., Gopakumar, L. R., Kumaran, A. K., Chatterjee, N. S., Soman, V., Peeralil, S., . . . Nagarajarao, R. C. (2021). Encapsulation and protection of omega-3-rich fish oils using food-grade delivery systems. *Foods, 10*(7), 1566.
40. Wang, J. (2020). *Complex coacervation between proteins and polysaccharides for the encapsulation of active molecules.* Université de Lyon,
41. Weinbreck, F., Minor, M., & De Kruif, C. (2004). Microencapsulation of oils using whey protein/gum arabic coacervates. *Journal of microencapsulation, 21*(6), 667-679.
42. Xiong, W., Ren, C., Tian, M., Yang, X., Li, J., & Li, B. (2017). Complex coacervation of ovalbumin-carboxymethylcellulose assessed by isothermal titration calorimeter and rheology: Effect of ionic strength and charge density of polysaccharide. *Food Hydrocolloids, 73*, 41-50.
43. Yang, Y., Anvari, M., Pan, C.-H., & Chung, D. (2012). Characterisation of interactions between fish gelatin and gum arabic in aqueous solutions. *Food Chemistry, 135*(2), 555-561.

44. Yun, P., Devahastin, S., & Chiewchan, N. (2021). Microstructures of encapsulates and their relations with encapsulation efficiency and controlled release of bioactive constituents: A review. *Comprehensive Reviews in Food Science and Food Safety*, *20*(2), 1768-1799.
45. Zuanon, L. A. C., Malacrida, C. R., & Telis, V. R. N. (2013). Production of turmeric Oleoresin microcapsules by complex Coacervation with gelatin–gum A rabic. *Journal of Food Process Engineering*, *36*(3), 364-373.

Figure captions

Figure 1. Effect of pH on zeta potential of FG and SSG dispersions.

Figure 2.Turbidity Values of FG and SSG, and Mixed Dispersions at Different pH Values, Concentrations (0.15% and 0.45%), with FG to SSG Ratio of 1:1.

Figure 3. Turbidity values and Yield at different FG to SSG ratios.

Figure 4. FG-SSG complex coacervates observed through light microscopy as a function of pH. (A) pH 5.4; (B) pH 4.5; (C) pH 4.2; (D) pH 3.8; (E) pH 3; (F) pH 2.

Figure 5. Scanning Electron Microscope (SEM) Pictures of Broken Surfaces of Freeze-Dried Complex Coacervates. (a) 100 µm, (b) 20 µm, (c) 10 µm, (d) 1 µm.